

pubs.acs.org/macroletters Letter

Bottlebrush Polymer Excipients Enhance Drug Solubility: Influence of End-Group Hydrophilicity and Thermoresponsiveness

Monica L. Ohnsorg, Paige C. Prendergast, Lindsay L. Robinson, Matthew R. Bockman, Frank S. Bates,* and Theresa M. Reineke*



Cite This: ACS Macro Lett. 2021, 10, 375-381



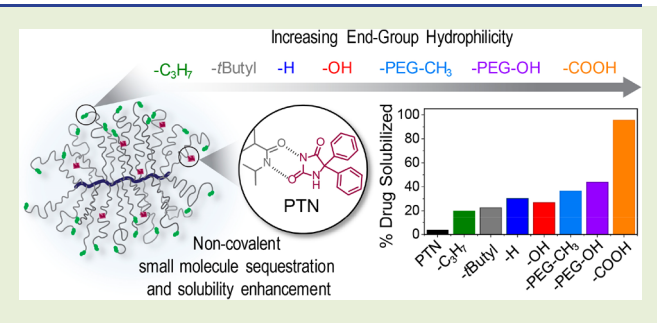
ACCESS

Metrics & More

Article Recommendations

s Supporting Information

ABSTRACT: Bottlebrush polymers have great potential as vehicles to noncovalently sequester, stabilize, and deliver hydrophobic small molecule actives. To this end, we synthesized a poly(*N*-isopropylacrylamide-*stat-N,N*-dimethylacrylamide) bottlebrush copolymer using ring-opening metathesis polymerization and developed a facile method to control the thermoresponsive properties using postpolymerization modification. Six increasingly hydrophilic end-groups were installed, yielding cloud point temperature control over a range of 22–42 °C. Solubility enhancement of the antiseizure medication, phenytoin, increased significantly with the hydrophilicity



of the end-group moiety. Notably, carboxylated bottlebrush copolymers solubilized formulations with higher drug loadings than linear copolymers because they exist as unimolecular nanoparticles with a synthetically defined density of polymer chains that are more stable in solution. This work provides the first investigation of bottlebrush polymers for hydrophobic noncovalent sequestration and solubilization of pharmaceuticals.

olymer excipients are inactive ingredients included in pill formulations that are frequently, but not exclusively, used to sequester small molecules and larger payloads through noncovalent interactions with active pharmaceutical ingredients (APIs),^{1,2} proteins,³⁻⁵ and polynucelotides.⁶ In oral, intravenous, or intramuscular administration, the polymer works with the active ingredients as a stabilizer, both on the shelf and in vivo. Although oral drug delivery is the most common form of medication administration, over 60% of APIs in the pharmaceutical pipeline are impacted by gastrointestinal track insolubility, yet, if solubilized, would have adequate permeability across the epithelial lining. Such APIs are categorized by the Biopharmaceutical Classification System (BCS) as Class II⁷ and can be solubilized with polymer excipients using a polymer-amorphous spray-dried dispersion (PASD) in which the amorphous API is suspended in a polymer matrix facilitating rapid dissolution and sustained solubility in aqueous media.8 Common classes of linear polymers used as excipients are cellulose-based, 9,10 polyvinylpyrrolidones, ^{11,12} poly(ethylene oxide), ¹³ and poly(acrylic acid).¹⁴ Many have been well studied with respect to the micro- and nanoscale interactions with APIs during dissolution. 15-17 However, the exploration of these important materials has been limited in the chemical and architectural scope. This has hindered the development of effective excipient-API pairs and, hence, the performance and commercialization of numerous important drug candidates.

Bottlebrush polymers are composed of side chains graftedto, -from, or -through a polymer backbone to form comb, globular, or worm-like architectures. 18 These macromolecules show unique and promising properties for many applications ranging from surface modification 19 and energy storage 20 to hydrogels^{21,22} and therapeutic delivery.^{23–28} Bottlebrushes present a well-defined and tunable synthetic platform, offering control over the density, ²⁹⁻³¹ monomer composition, ³² and conformation³³ of the side chains. Ring-opening metathesis polymerization (ROMP) of norbornene-functionalized macromonomers (MMs) affords an efficient route to globular macromolecular structures with densely packed side chains with diverse compositions,³⁴ including hydrophobic,^{35–37} hydrophilic,^{24,36} and thermoresponsive^{38,39} moieties. Therapeutics and imaging labels can be covalently attached to bottlebrush architectures using established coupling chemistries^{23-25,27} to achieve controlled release in the presence of the appropriate stimulus.²⁸ While bottlebrush polymers have been shown to be successful delivery vehicles through covalent conjugation, the interactions of such macromolecules with small molecules through noncovalent interactions is not well studied. 40 Understanding the ability of these systems to serve as supramolecular hosts could enable the development of

Received: December 23, 2020 Accepted: February 1, 2021 Published: February 16, 2021





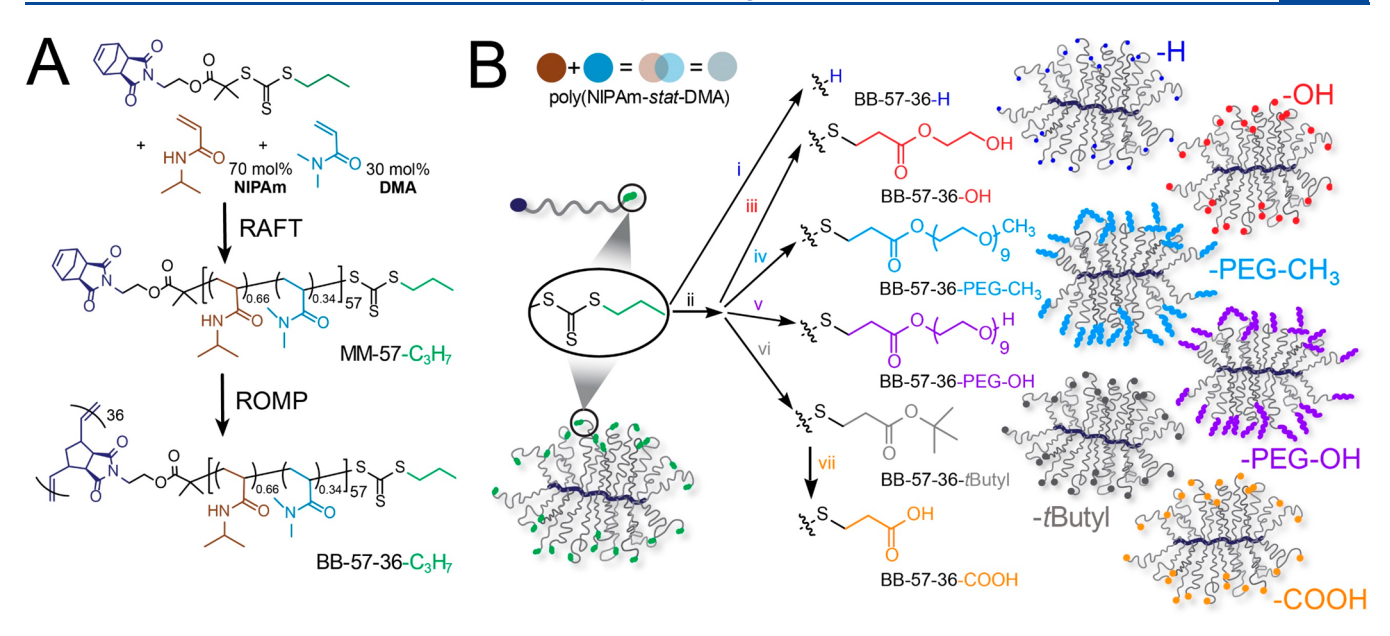


Figure 1. (A) Synthetic scheme for macromonomer MM-57- C_3H_7 and bottlebrush BB-57-36- C_3H_7 . RAFT polymerization was run to 80% conversion in 1,4-dioxane with 0.05 equiv of AIBN at 70 °C. ROMP was run in dichloromethane (DCM) with Grubb's 3rd generation catalyst. (B) Postpolymerization modification of MM-57- C_3H_7 and BB-57-36- C_3H_7 . The color code defines gray as poly(NIPAm-stat-DMA) in cartoon representations, (i) toluene/methanol (70:30), 1-ethylpiperidine hypophosphite, blue light (450 nm), 25 °C, 4 days, (ii) tetrahydrofuran, tris(2-carboxyethyl)phosphine hydrochloride, n-propylamine, 23 °C, 1 h, (iii) hydroxy ethyl acrylate, 23 °C, 14 h, (iv) poly(ethylene glycol) methyl ether acrylate, 23 °C, 14 h, (v) poly(ethylene glycol) hydroxy ether acrylate, 23 °C, 14 h, (vi) tert-butyl acrylate, 23 °C, 14 h, (vii) trifluoroacetic acid, DCM, 23 °C, 5 h.

Table 1. Summary of Physical and Solution Characterization of Linear (PND) Controls and End-Group Modified Macromonomer (MM) and Bottlebrush (BB) Polymers

sample	$mol \%^a (N/D)$	M_n^b (kDa)	$M_{\rm w, SEC}^{b}$ (kDa)	$\overline{\mathcal{D}}^{\boldsymbol{b}}$	$T_{\rm cp}^{c}$ (°C)	$R_{h,25} \circ_{C}^{d} (nm)$	$\mu_2/\Gamma^{2,d}$	density e (mg/mL)
1 PA-PND-245-C ₃ H ₇	65/35	31 ^f	30	1.11	39	5.5, 34.0	0.29, 0.22	
2 PA-PND-61-C ₃ H ₇	66/34	7.3^{f}	7.0	1.02	44	2.5	0.18	
3 PA-PND-62-C ₁₂ H ₂₅	66/34	7.1^{f}	7.2	1.02	50	7.4 ^h	0.21 ^h	74 ⁴³
4 CA-PND-62-C ₁₂ H ₂₅	66/34	7.0 ^f	7.2	1.02	51	7.2	0.12	
5 CP-PND-72-C ₁₂ H ₂₅	64/36	9.0 ^f	8.3	1.02	38	7.9	0.04	
$MM-57-C_3H_7$	66/34	6.2^{f}	6.9	1.04	31	1.6	0.11	
MM-57-H	66/34	6.3	6.6	1.04	37	2.7, 11.7	0.29, 0.22	
MM-57-OH	66/34	6.4	6.7	1.04	41	2.6	0.31	
MM-57-PEG-CH ₃	66/34	6.5	6.7	1.04	44	2.5	0.17	
MM-57-PEG-OH	66/34	6.6	7.0	1.05	43	2.3, 47.6	0.06, 0.11	
MM-57-tButyl	66/34	6.3	6.4	1.03	38	2.2	0.22	
MM-57-COOH	66/34	6.4	6.6	1.03	43	2.4	0.34	
BB-57-36- C_3H_7	66/34	240	280	1.15	22	$9.5^{g,h}$	$0.11^{g,h}$	105 ^g
BB-57-36-H	66/34	230	260	1.15	35	9.6 ^h	0.07^{h}	101
BB-57-36-OH	66/34	240	280	1.19	35	10.0 ^h	0.09^{h}	91
BB-57-36-PEG-CH ₃	66/34	240	290	1.20	39	10.0 ^h	0.07^{h}	89
BB-57-36-PEG-OH	66/34	240	280	1.15	39	9.7^{h}	0.13^{h}	99
BB-57-36- <i>t</i> Butyl	66/34	230	270	1.15	29	9.6 ^h	0.07 ^h	100
BB-57-36-COOH	66/34	230	$250 \ (250^i)$	1.07	42	9.8 ^h	0.08 ^h	96

 a1 H NMR ratio of peak integrations at 1H at 4.00 ppm to 6H at 3.25 ppm. b SEC-MALS in DMF with 0.05 M LiBr. c Cloud point measurements determined at 80% transmittance. d DynaPro plate reader DLS – regularization fit (9 mg/mL). e Calculated using eq S1. f M_n by 1 H NMR in CDCl₃. g Measured at 20 $^{\circ}$ C. h Multiangle DLS 2nd cumulant fit (1 mg/mL). i M_w calculated by SLS.

highly tunable, multivalent vehicles to enhance solubility, release, and/or delivery of intractable active molecules through noncovalent interactions.

Hydrophilic and thermoresponsive polyacrylamide-containing copolymers, 41,42 such as poly(*N*-isopropylacrylamide-*stat-N,N*-dimethylacrylamide) (poly(NIPAm-*stat-DMA*) or PND) have been shown to outperform standard excipients, such as hydroxypropyl methylcellulose acetate succinate (HPMCAS)

when applied to rapidly crystallizing small molecule therapeutics. ⁴¹ This has been attributed to the balancing of three synergistic effects: (*i*) inhibition of crystallization by NIPAm repeat units, (*ii*) enhanced solubility imparted by the DMA at the optimal ratio of 65:35 NIPAm:DMA, and (*iii*) formation of nanoaggregates that host the drug during dissolution. ⁴¹ Tactics to further increase excipient efficacy generally rely on improving the rate of dissolution, self-

assembly, and colloidal stability of drug-rich nanoparticles, which form during the dissolution process. ¹⁶ Previous work increased the strength of polymer—API noncovalent interactions with such polyacrylamide copolymers by increasing the density of polymer chains within a defined volume such as the corona of block copolymer micelles ⁴³ or using nanogel ⁴⁴ architectures. Bottlebrush polymers offer a robust design space, decoupling the variables of polymer chain chemistry, density, and end-group functionality from the typical constraints of micelle self-assembly, as a synthetically tunable macromolecular scaffold.

In this work we hypothesized that bottlebrush polymers would promote effective noncovalent sequestration and retention of small molecule APIs as unimolecular nanoparticles while affording more architectural control and stability over self-assembled micelles, thus, directly improving excipient solubilization effectiveness. Herein, a poly(NIPAm-stat-DMA) bottlebrush copolymer was synthesized using graftingthrough methods (Figure 1A) and was used as a template to isolate the effects of end-group functionality while keeping molecular weight, monomer composition, and polymer architecture (chain density) constant. We synthesized a ROMP-active chain transfer agent (CTA) with a propyl (-C₃H₇) Z-group (Scheme S1 and Figure S1-S4) in an effort to initially reduce the hydrophobic contribution of the endgroups. Shown in Figure 1A, the MM-57-C₃H₇, polymerized using reversible addition-fragmentation chain transfer (RAFT) with the ROMP-active CTA, were stitched together through ROMP (>95% conversion) to form the bottlebrush template (BB-N_{sc}-N_{bb}-Z) with a side-chain degree of polymerization (N_{sc}) of 57 and a backbone degree of polymerization $(N_{\rm bb})$ of 36 with propyl Z-groups, BB-57-36-C₃H₇ (Schemes S2-S6 and Figures S5-S11). Both MM-57-C₃H₇ and BB-57-36-C₃H₇ were end-group modified post-RAFT and post-ROMP, respectively (Figure 1B, Schemes S7 and S8 and Figures S12-S27). The end-group functionality was systematically altered by either fully removing the trithiocarbonate (-H) using photoinduced chain transfer in the presence of a proton donor⁴⁵ or thia-Michael addition to install a spectrum of acrylates, 46 yielding the following end-groups: hydroxyl (-OH), methyl-PEG (-PEG-CH₃), hydroxy-PEG (-PEG-OH), tert-butyl (-t-butyl), and carboxylic acid (-COOH). The dense bottlebrush architectures were compared to five linear PND controls polymerized via RAFT with four distinct CTAs (Table 1, Scheme S9, and Figures S28-S33): (1) propionic acid(PA)-PND-245-C₃H₇, (2) PA-PND-61-C₃H₇, (3) PA-PND-62-C₁₂H₂₅, (4) cyano-acid(CA)-PND-62-C₁₂H₂₅, and (5) cyano-propyl(CP)-PND-72- $C_{12}H_{25}$.

The influence of end-group functionality on the bottlebrush (BB) polymers was assessed as a function of cloud point temperature ($T_{\rm cp}$), solution structure, and density and compared to the linear copolymer analogues (1–5) and end-group modified macromonomers (MM; see additional discussion, Figures S34–S45, Tables S2–S4). The $T_{\rm cp}$ of BB-57-36-C₃H₇ decreased to 22 °C due to the increased molecular weight and hydrophobic contributions from 36 propyl end-groups compared to the linear copolymer controls 1–5 ($T_{\rm cp} \geq$ 38 °C). Because the molecular weight and composition of the side chains remained constant, Z-groups were responsible for the incremental increase in $T_{\rm cp}$ with increasing hydrophilicity, -tbutyl < -H \approx -OH < -PEG-CH₃ \approx -PEG-OH < -COOH, where $T_{\rm cp} =$ 42 °C for BB-57-36-COOH (Table 1, Figure 2A). Therefore, using end-group modification

alone, we systematically tuned the $T_{\rm cp}$ of the thermoresponsive bottlebrush polymers spanning a range of 22–42 °C.

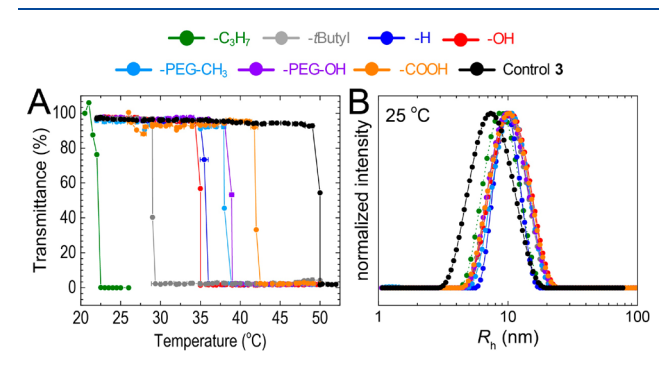


Figure 2. (A) Transmittance data for the end-group modified BB and control 3 upon heating: 9 mg/mL sample in PBS pH 6.5. (B) $R_{\rm h}$ distributions of BB-57-36-Z and control 3 at 1 mg/mL in PBS pH 6.5 at 25 °C (BB-C₃H₇ measured at 20 °C) calculated using regularized positive exponential sum (REPES) Laplace inversion route analysis. ⁴⁷

Bottlebrush polymers are enticing candidates to create synthetically fixed unimolecular micelle-like or globular nanoparticles. The hydrodynamic radius (R_h) of BB-57-36-C₃H₇ was measured at 20 °C to demonstrate that, below its cloud point ($T_{cp} = 22$ °C), the particles with a $R_h = 9.5$ nm did not aggregate in solution (Table 1 and Figure 2B). Each Zgroup variation of BB-57-36-C₃H₇ was measured to have a polydispersity index (PDI) less than 0.15, indicating they exist as well-defined, monodisperse unimers in solution with a R_h = 9.6-10 nm (Table 1, Figure 2B, Figures S43 and S44). This confirms that bottlebrushes were not coupled together through disulfide bond formation or other radical side reactions during end-group modification. The dodecyl Z-groups drive control 3 to form a monomodal population of micelles with a $R_h = 7.4$ nm (Figure 2B). Therefore, control 3 could be directly compared to the globular macromolecular bottlebrushes (shape factor $^{48,49} = 0.96$, Figure S45) as a noncovalent supramolecular architecture. Due to a T_{cp} above 37 °C, BB-57-36-PEG-CH₃, -PEG-OH, and -COOH maintained monomodal populations in solution at 37 °C (Figure S40) with minimal change in R_h from 25 °C. We estimated the average density (ρ_{BB}) of each end-group modified bottlebrush to be between 89 and 105 mg/mL (Table 1, see eq S1), replicating the optimal density range exhibited by previous work in the drug delivery field with micelles and cross-linked nanogels. 43,44,50-Based on these data, we hypothesized that the bottlebrush excipient architecture should facilitate sustained solubilization at higher drug loading due to a high density of polymer chains promoting noncovalent associations with APIs through the NIPAm moieties.

We examined solubility enhancement performance with a model BCS Class II API, phenytoin (PTN), an anticonvulsant on the World Health Organization's list of essential medicines 53 (log $P=2.14,^{54}$ $T_{\rm m}=295$ °C). Each BB-57-36-Z, MM-57-Z, and controls 1–5 were spray dried with 10 wt % of PTN (confirmed by synchrotron WAXS, Figure S46), and the concentration of the solubilized PTN in the fasted-state simulated intestinal fluid (FaSSIF) during the dissolution experiment was evaluated using high-pressure liquid chromatography at 4, 10, 20, 40, 90, 180, and 360 min (at 25 and 37 °C). A complete discussion of the dissolution results with linear controls and macromonomers can be found in Figures

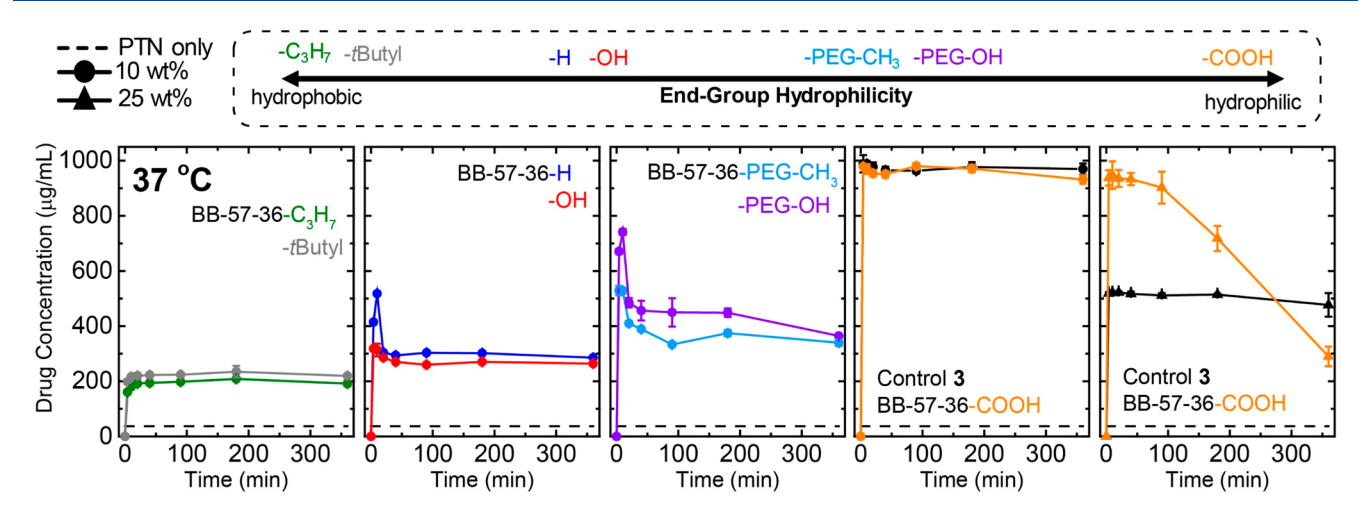


Figure 3. Dissolution results for the BB-57-36-Z and control 3 with 10 wt % (circles) and 25 wt % (triangles) PTN in FaSSIF pH 6.5 at 37 °C, arranged in order of most hydrophobic to hydrophilic Z-group.

S47-S57. At 37 °C (Figure 3), the bottlebrush dissolution performance improved incrementally with increasing hydrophilicity of the Z-group (from -C₃H₇ to -COOH), mirroring the trend in $T_{\rm cp}$ shown in Figure 2A. It was observed that $T_{\rm cp}$ with respect to the targeted delivery temperature played an important role in determining PASD solubilization effectiveness (see dissolution results at 25 °C, Figure S57, and Extra Discussion - Drug Dissolution Performance in the SI). Both PEGylated bottlebrush polymers had a T_{cp} above 37 °C and showed burst-like release profiles, prompting the following question: why is PEGylation not enough to fully solubilize and maintain 1000 μ g/mL in solution for 6 h as with BB-57-36-COOH? Static light scattering (SLS) measurements revealed that the second virial coefficient (A2) measured at 25 °C was four times larger for BB-57-36-COOH versus BB-57-36-PEG-CH₃ (Table S4 and Figure S45). Therefore, carboxylic acid groups increased the solvent quality for this bottlebrush facilitating rapid dissolution and sustained solubility of the PASD in FaSSIF. The top performing polymer excipients were control 3 and BB-57-36-COOH, which both solubilized amorphous API by forming ~20 nm drug-loaded particles that were stable in solution for 6 h (Figure 4A, DLS studies described in Figures \$58 and \$59). Therefore, both were spraydried at 25 wt % PTN loading.

The dissolution results for control 3 and BB-57-36-COOH with 25 wt % PTN loading at 37 °C are shown in Figure 3. Consistent with previous studies, 41,43 the linear control was unable to solubilize greater than 600 μ g/mL of PTN. For the BB-57-36-COOH PASD, we observed full solubilization of the targed 1000 μ g/mL of PTN at 25 wt % loading for up to 90 min. To the best of our knowledge, this is the first report of full solubilization of PTN from a PASD at 25 wt % drug loading and highlights the importance of polymer architecture through tailoring the density of chains in enhancing solubility through the noncovalent sequestration of small molecule APIs. Although crystallization occurred over time due to the transition from polymer-API to API-API noncovalent interactions leading to drug crystal nucleation and growth, BB-57-36-COOH can fully solubilize 1000 ug/mL of the API at early time points. DLS studies (Figure 4B) during dissolution revealed that BB-57-36-COOH solubilized and stabilized amorphous PTN monomodal drug-loaded nanoparticles (~26 nm) despite crystallization over time evidenced

by polarized light microscopy (Figure S73). In contrast, control 3 could not stabilize 25 wt % of PTN without significant aggregation and polymer-drug separation (Figure 4B,C and see Figure S71 for polarized light microscopy). Overall, these data show that the bottlebrushes can sequester small molecules as distinct unimolecular nanoparticles (Figure 4C) that, due to a synthetically defined density of polymer chains, are more stable in solution, despite higher loadings of hydrophobic small molecules, making them superior to linear polymer excipients.

Interestingly, from a stoichiometric perspective, we estimate that each BB-57-36-COOH hosts 331 PTN molecules and each polymer chain of control 3 needs to stabilize 10 PTN molecules at 25 wt % drug loading. We also consider the number of NIPAm repeat units per PTN molecule in each system with respect to de Genne's theory of *n*-clustering⁵⁵ in which NIPAm units can form hydrophobic environments (without a temperature driven transition) through intermolecular associations between the isopropyl groups of "n" NIPAm repeat units. At 25 wt %, there are four NIPAm repeat units per PTN molecule in each system. The lower limit of "n" in NIPAm containing copolymers has been experimentally determined to be about three or four. 56 Therefore, since not every NIPAm repeat unit exists in a triad or quartet along a statistical copolymer chain, the ratio of PTN molecules to nclusters in these systems is slightly more than 1:1. We hypothesize that the excess PTN molecules overwhelm the nclusters present within the linear PND excipient and crystallization occurs. However, because the bottlebrush architecture synthetically fixes the density of polymer chains within a defined volume, the ratio of PTN molecules to nclusters can be shifted toward unity for a short period of time facilitating the 90 min of full dissolution seen in Figure 3. This n-clustering limit of four NIPAm repeat units per drug molecule in a PASD formulation could be used to predict the upper limit of drug solubilization effectiveness of PND excipients with other small molecule APIs.

In conclusion, we have presented the first study using bottlebrush polymers for the physical sequestration and solubilization of hydrophobic pharmaceuticals enabled through postpolymerization end-group modification of a thermoresponsive bottlebrush copolymer template. Through end-group modification only, we systematically increased the hydro-

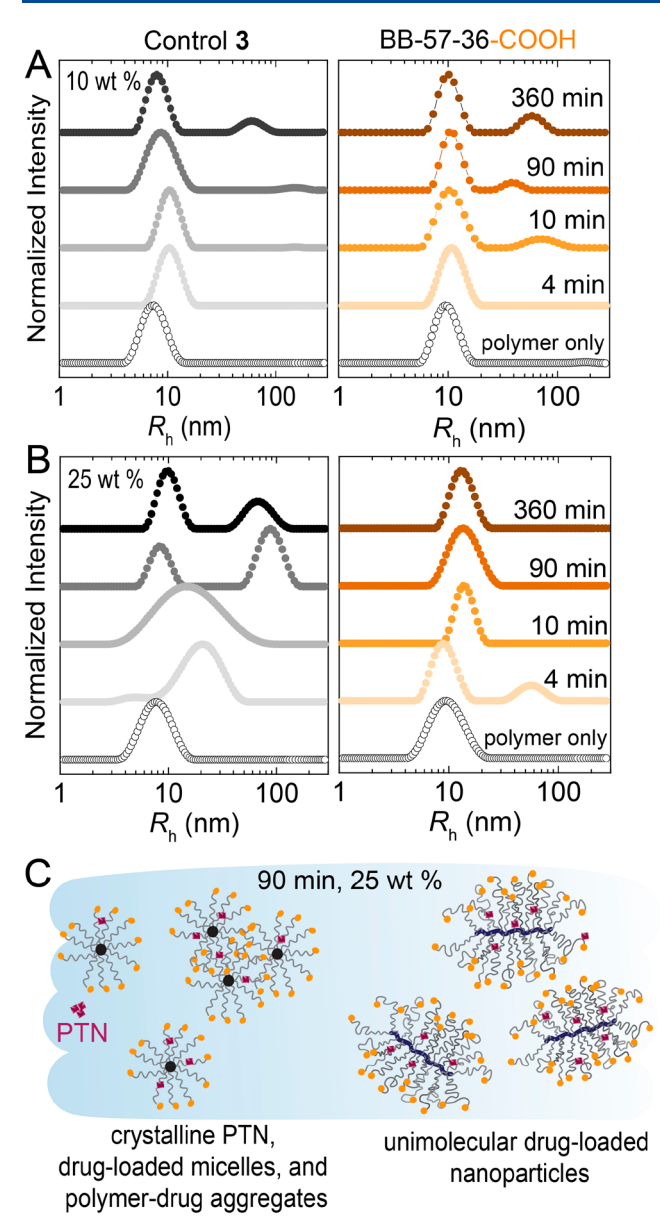


Figure 4. Dynamic light scattering R_h distributions during dissolution run in PBS at 37 °C for control 3 and BB-57-36-COOH with (A) 10 wt % PTN and (B) 25 wt % PTN at 4, 10, 90, and 360 min. Polymer only (open circles) samples were measured at 9 mg/mL in PBS at 37 °C. (C) Illustration of the drug—polymer species present in solution at 90 min during dissolution with 25 wt % PTN.

philicity of the bottlebrush polymer, incrementally increasing the solubility enhancement of each bottlebrush with the model API, PTN. The carboxylated bottlebrush out-performed the linear copolymers at 25 wt % drug loadings. This superior performance was attributed to the synthetically fixed density of bottlebrush copolymer side chains. Bottlebrush architectures are ideal vehicles for the physical encapsulation of hydrophobic small molecules and have great potential for future applications in sequestration, stabilization, and delivery of a multitude of important active molecules.

ASSOCIATED CONTENT

Supporting Information

(PDF) The Supporting Information is available free of charge at https://pubs.acs.org/doi/10.1021/acsmacrolett.0c00890.

General information, materials, experimental procedures, ¹H and ¹³C NMR spectroscopy, SEC, transmittance measurements, dynamic and static light scattering, density calculations, wide-angle X-ray scattering, dissolution results, and polarized light microscopy images (PDF)

AUTHOR INFORMATION

Corresponding Authors

Frank S. Bates — Department of Chemical Engineering and Material Science, University of Minnesota, Minneapolis, Minnesota 55455, United States; oorcid.org/0000-0003-3977-1278; Email: bates001@umn.edu

Theresa M. Reineke — Department of Chemistry, University of Minnesota, Minneapolis, Minnesota 55455, United States; orcid.org/0000-0001-7020-3450; Email: treineke@umn.edu

Authors

Monica L. Ohnsorg — Department of Chemistry, University of Minnesota, Minneapolis, Minnesota 55455, United States; orcid.org/0000-0002-7616-3880

Paige C. Prendergast — Department of Chemistry, University of Minnesota, Minneapolis, Minnesota 55455, United States Lindsay L. Robinson — Department of Chemistry, University of Minnesota, Minneapolis, Minnesota 55455, United States Matthew R. Bockman — Department of Chemistry, University of Minnesota, Minneapolis, Minnesota 55455, United States

Complete contact information is available at: https://pubs.acs.org/10.1021/acsmacrolett.0c00890

Author Contributions

All authors have given approval to the final version of the manuscript.

Notes

The authors declare no competing financial interest.

ACKNOWLEDGMENTS

This work acknowledges the financial support of Dow Chemical Company and DuPont Chemical Company. M.L.O. acknowledges funding support by the National Science Foundation Graduate Research Fellowship under Grant No. 00039202. P.C.P. was supported (partially) by the Research Experiences for Undergraduates (REU) Program of the National Science Foundation under Award Number DMR-1559833 and through the University of Minnesota MRSEC under Award Number DMR-2011401. WAXS measurements were collected at the Advance Photon Source (APS), Sector 5 (DuPont-Northwestern-Dow Collaborative Access Team, DND-CAT). DND-CAT is supported by E.I. DuPont de Nemours & Co., The Dow Chemical Company, and Northwestern University. Use of the APS, an Office of Science User Facility operated for the U.S. Department of Energy (DOE) Office of Science by Argonne National Laboratory, was supported by the U.S. DOE under Contract No. DE-AC02-06CH11357. We also thank Nicholas Van Zee for his assistance with the polarized light microscopy, which was carried out in the College of Science and Engineering Characterization Facility, University of Minnesota, which has received capital equipment funding from the NSF through the UMN MRSEC program under Award Number DMR 2011401.

■ REFERENCES

- (1) Warren, D. B.; Benameur, H.; Porter, C. J. H.; Pouton, C. W. Using Polymeric Precipitation Inhibitors to Improve the Absorption of Poorly Water-Soluble Drugs: A Mechanistic Basis for Utility. *J. Drug Target.* **2010**, *18* (10), 704–731.
- (2) Ting, J. M.; Porter, W. W.; Mecca, J. M.; Bates, F. S.; Reineke, T. M. Advances in Polymer Design for Enhancing Oral Drug Solubility and Delivery. *Bioconjugate Chem.* **2018**, *29*, 939–952.
- (3) Katz, J. S.; Nolin, A.; Yezer, B. A.; Jordan, S. Dynamic Properties of Novel Excipient Suggest Mechanism for Improved Performance in Liquid Stabilization of Protein Biologics. *Mol. Pharmaceutics* **2019**, *16*, 282–291.
- (4) Katz, J. S.; Tan, Y.; Kuppannan, K.; Song, Y.; Brennan, D. J.; Young, T.; Yao, L.; Jordan, S. Amino-Acid-Incorporating Nonionic Surfactants for Stabilization of Protein Pharmaceuticals. *ACS Biomater. Sci. Eng.* **2016**, *2*, 1093–1096.
- (5) Hanson, M. G.; Katz, J. S.; Ma, H.; Putterman, M.; Yezer, B. A.; Petermann, O.; Reineke, T. M. Effects of Hydrophobic Tail Length Variation on Surfactant-Mediated Protein Stabilization. *Mol. Pharmaceutics* **2020**, *17*, 4302–4311.
- (6) Van Bruggen, C.; Hexum, J. K.; Tan, Z.; Dalal, R. J.; Reineke, T. M. Nonviral Gene Delivery with Cationic Glycopolymers. *Acc. Chem. Res.* **2019**, *52*, 1347–1358.
- (7) Amidon, G. L.; Lennernäs, H.; Shah, V. P.; Crison, J. R. A Theoretical Basis for a Biopharmaceutic Drug Classification: The Correlation of in Vitro Drug Product Dissolution and in Vivo Bioavailability. *Pharm. Res.* 1995, 12 (3), 413–420.
- (8) Baghel, S.; Cathcart, H.; O'Reilly, N. J. Polymeric Amorphous Solid Dispersions: A Review of Amorphization, Crystallization, Stabilization, Solid-State Characterization, and Aqueous Solubilization of Biopharmaceutical Classification System Class II Drugs. *J. Pharm. Sci.* **2016**, *105* (9), 2527–2544.
- (9) Chavan, R. B.; Rathi, S.; Jyothi, V. G. S. S.; Shastri, N. R. Cellulose Based Polymers in Development of Amorphous Solid Dispersions. *Asian J. Pharm. Sci.* **2019**, *14*, 248–264.
- (10) Wilson, V. R.; Lou, X.; Osterling, D. J.; Stolarik, D. A. F.; Jenkins, G. J.; Nichols, B. L. B.; Dong, Y.; Edgar, K. J.; Zhang, G. G. Z.; Taylor, L. S. Amorphous Solid Dispersions of Enzalutamide and Novel Polysaccharide Derivatives: Investigation of Relationships between Polymer Structure and Performance. *Sci. Rep.* **2020**, *10*, 18535.
- (11) Kothari, K.; Ragoonanan, V.; Suryanarayanan, R. The Role of Polymer Concentration on the Molecular Mobility and Physical Stability of Nifedipine Solid Dispersions. *Mol. Pharmaceutics* **2015**, *12*, 1477–1484.
- (12) Franco, P.; De Marco, I. The Use of Poly(N-Vinyl Pyrrolidone) in the Delivery of Drugs: A Review. *Polymers (Basel, Switz.)* **2020**, *12*, 1114.
- (13) Broman, E.; Khoo, C.; Taylor, L. S. A Comparison of Alternative Polymer Excipients and Processing Methods for Making Solid Dispersions of a Poorly Water Soluble Drug. *Int. J. Pharm.* **2001**, 222, 139–151.
- (14) Kothari, K.; Ragoonanan, V.; Suryanarayanan, R. The Role of Drug-Polymer Hydrogen Bonding Interactions on the Molecular Mobility and Physical Stability of Nifedipine Solid Dispersions. *Mol. Pharmaceutics* **2015**, *12*, 162–170.
- (15) Ricarte, R. G.; Van Zee, N. J.; Li, Z.; Johnson, L. M.; Lodge, T. P.; Hillmyer, M. A. Recent Advances in Understanding the Microand Nanoscale Phenomena of Amorphous Solid Dispersions. *Mol. Pharmaceutics* **2019**, *16*, 4089–4103.
- (16) Van Zee, N. J.; Hillmyer, M. A.; Lodge, T. P. Role of Polymer Excipients in the Kinetic Stabilization of Drug-Rich Nanoparticles. *ACS Appl. Bio Mater.* **2020**, *3*, 7243–7254.
- (17) Li, N.; Taylor, L. S. Microstructure Formation for Improved Dissolution Performance of Lopinavir Amorphous Solid Dispersions. *Mol. Pharmaceutics* **2019**, *16*, 1751–1765.
- (18) Verduzco, R.; Li, X.; Pesek, S. L.; Stein, G. E. Structure, Function, Self-Assembly, and Applications of Bottlebrush Copolymers. *Chem. Soc. Rev.* **2015**, *44*, 2405–2420.

- (19) Li, X.; Prukop, S. L.; Biswal, S. L.; Verduzco, R. Surface Properties of Bottlebrush Polymer Thin Films. *Macromolecules* **2012**, 45, 7118–7127.
- (20) Bates, C. M.; Chang, A. B.; Momcilovic, N.; Jones, S. C.; Grubbs, R. H. ABA Triblock Brush Polymers: Synthesis, Self-Assembly, Conductivity, and Rheological Properties. *Macromolecules* **2015**, *48*, 4967–4973.
- (21) Keith, A. N.; Vatankhah-Varnosfaderani, M.; Clair, C.; Fahimipour, F.; Dashtimoghadam, E.; Lallam, A.; Sztucki, M.; Ivanov, D. A.; Liang, H.; Dobrynin, A. V.; Sheiko, S. S. Bottlebrush Bridge between Soft Gels and Firm Tissues. *ACS Cent. Sci.* **2020**, *6*, 413–419.
- (22) Daniel, W. F. M.; Burdyńska, J.; Vatankhah-Varnoosfaderani, M.; Matyjaszewski, K.; Paturej, J.; Rubinstein, M.; Dobrynin, A. V.; Sheiko, S. S. Solvent-Free, Supersoft and Superelastic Bottlebrush Melts and Networks. *Nat. Mater.* **2016**, *15*, 183–189.
- (23) Müllner, M.; Dodds, S. J.; Nguyen, T. H.; Senyschyn, D.; Porter, C. J. H.; Boyd, B. J.; Caruso, F. Size and Rigidity of Cylindrical Polymer Brushes Dictate Long Circulating Properties in Vivo. *ACS Nano* **2015**, *9* (2), 1294–1304.
- (24) Johnson, J. A.; Lu, Y. Y.; Burts, A. O.; Xia, Y.; Durrell, A. C.; Tirrell, D. A.; Grubbs, R. H. Drug-Loaded, Bivalent-Bottle-Brush Polymers by Graft-through ROMP. *Macromolecules* **2010**, *43* (24), 10326–10335.
- (25) Lv, F.; Liu, D.; Cong, H.; Shen, Y.; Yu, B. Synthesis, Self-Assembly and Drug Release Behaviors of a Bottlebrush Polymer-HCPT Prodrug for Tumor Chemotherapy. *Colloids Surf., B* **2019**, 181, 278–284.
- (26) Li, H.; Liu, H.; Nie, T.; Chen, Y.; Wang, Z.; Huang, H.; Liu, L.; Chen, Y. Molecular Bottlebrush as a Unimolecular Vehicle with Tunable Shape for Photothermal Cancer Therapy. *Biomaterials* **2018**, 178, 620–629.
- (27) Wang, D.; Lin, J.; Jia, F.; Tan, X.; Wang, Y.; Sun, X.; Cao, X.; Che, F.; Lu, H.; Gao, X.; Shimkonis, J. C.; Nyoni, Z.; Lu, X.; Zhang, K. Bottlebrush-Architectured Poly(Ethylene Glycol) as an Efficient Vector for RNA Interference in Vivo. Sci. Adv. 2019, 5 (2), eaav9322.
- (28) Müllner, M. Molecular Polymer Brushes in Nanomedicine. *Macromol. Chem. Phys.* **2016**, 217 (20), 2209–2222.
- (29) Lin, T.-P.; Chang, A. B.; Chen, H.-Y.; Liberman-Martin, A. L.; Bates, C. M.; Voegtle, M. J.; Bauer, C. A.; Grubbs, R. H. Control of Grafting Density and Distribution in Graft Polymers by Living Ring-Opening Metathesis Copolymerization. *J. Am. Chem. Soc.* **2017**, *139*, 3896–3903.
- (30) Chang, A. B.; Lin, T. P.; Thompson, N. B.; Luo, S. X.; Liberman-Martin, A. L.; Chen, H. Y.; Lee, B.; Grubbs, R. H. Design, Synthesis, and Self-Assembly of Polymers with Tailored Graft Distributions. *J. Am. Chem. Soc.* **2017**, *139*, 17683–17693.
- (31) Haugan, I. N.; Maher, M. J.; Chang, A. B.; Lin, T.-P.; Grubbs, R. H.; Hillmyer, M. A.; Bates, F. S. Consequences of Grafting Density on the Linear Viscoelastic Behavior of Graft Polymers. *ACS Macro Lett.* **2018**, *7*, 525–530.
- (32) Li, Z.; Ma, J.; Lee, N. S.; Wooley, K. L. Dynamic Cylindrical Assembly of Triblock Copolymers by a Hierarchical Process of Covalent and Supramolecular Interactions. *J. Am. Chem. Soc.* **2011**, 133, 1228–1231.
- (33) Pesek, S. L.; Li, X.; Hammouda, B.; Hong, K.; Verduzco, R. Small-Angle Neutron Scattering Analysis of Bottlebrush Polymers Prepared via Grafting-through Polymerization. *Macromolecules* **2013**, 46, 6998–7005.
- (34) Choinopoulos, I. Grubbs' and Schrock's Catalysts, Ring Opening Metathesis Polymerization and Molecular Brushes—Synthesis, Characterization, Properties and Applications. *Polymers (Basel, Switz.)* **2019**, *11*, 298–329.
- (35) Xia, Y.; Kornfield, J. A.; Grubbs, R. H. Efficient Synthesis of Narrowly Dispersed Brush Polymers via Living Ring-Opening Metathesis Polymerization of Macromonomers. *Macromolecules* **2009**, *42*, 3761–3766.
- (36) Li, Z.; Zhang, K.; Ma, J.; Cheng, C.; Wooley, K. L. Facile Syntheses of Cylindrical Molecular Brushes by a Sequential RAFT

- and ROMP "Grafting-Through" Methodology. J. Polym. Sci., Part A: Polym. Chem. 2009, 47, 5557-5563.
- (37) Radzinski, S. C.; Foster, J. C.; Chapleski, R. C.; Troya, D.; Matson, J. B. Bottlebrush Polymer Synthesis by Ring-Opening Metathesis Polymerization: The Significance of the Anchor Group. *J. Am. Chem. Soc.* **2016**, *138*, 6998–7004.
- (38) Li, X.; ShamsiJazeyi, H.; Pesek, S. L.; Agrawal, A.; Hammouda, B.; Verduzco, R. Thermoresponsive PNIPAAM Bottlebrush Polymers with Tailored Side-Chain Length and End-Group Structure. *Soft Matter* **2014**, *10*, 2008–2015.
- (39) Kang, J. J.; Jung, F. A.; Ko, C. H.; Shehu, K.; Barnsley, L. C.; Kohler, F.; Dietz, H.; Zhao, J.; Pispas, S.; Papadakis, C. M. Thermoresponsive Molecular Brushes with Propylene Oxide/Ethylene Oxide Copolymer Side Chains in Aqueous Solution. *Macromolecules* **2020**, *53*, 4068–4081.
- (40) Foster, J. C.; Varlas, S.; Couturaud, B.; Coe, Z.; O'Reilly, R. K. Getting into Shape: Reflections on a New Generation of Cylindrical Nanostructures' Self-Assembly Using Polymer Building Blocks. *J. Am. Chem. Soc.* **2019**, *141*, 2742–2753.
- (41) Ting, J. M.; Tale, S.; Purchel, A. A.; Jones, S. D.; Widanapathirana, L.; Tolstyka, Z. P.; Guo, L.; Guillaudeu, S. J.; Bates, F. S.; Reineke, T. M. High-Throughput Excipient Discovery Enables Oral Delivery of Poorly Soluble Pharmaceuticals. *ACS Cent. Sci.* **2016**, *2* (10), 748–755.
- (42) Mann, J. L.; Maikawa, C. L.; Smith, A. A. A.; Grosskopf, A. K.; Baker, S. W.; Roth, G. A.; Meis, C. M.; Gale, E. C.; Liong, C. S.; Correa, S.; Chan, D.; Stapleton, L. M.; Yu, A. C.; Muir, B.; Howard, S.; Postma, A.; Appel, E. A. An Ultrafast Insulin Formulation Enabled by High-Throughput Screening of Engineered Polymeric Excipients. Sci. Transl. Med. 2020, 12, eaba6676.
- (43) Li, Z.; Lenk, T. I.; Yao, L. J.; Bates, F. S.; Lodge, T. P. Maintaining Hydrophobic Drug Supersaturation in a Micelle Corona Reservoir. *Macromolecules* **2018**, *51* (2), 540–551.
- (44) Li, Z.; Van Zee, N. J.; Bates, F. S.; Lodge, T. P. Polymer Nanogels as Reservoirs to Inhibit Hydrophobic Drug Crystallization. *ACS Nano* **2019**, *13*, 1232–1243.
- (45) Carmean, R. N.; Figg, C. A.; Scheutz, G. M.; Kubo, T.; Sumerlin, B. S. Catalyst-Free Photoinduced End-Group Removal of Thiocarbonylthio Functionality. *ACS Macro Lett.* **2017**, *6* (2), 185–189.
- (46) Willcock, H.; O'Reilly, R. K. End Group Removal and Modification of RAFT Polymers. *Polym. Chem.* **2010**, *1*, 149–157.
- (47) Jakeš, J. Regularized Positive Exponential Sum (REPES) Program A Way of Inverting Laplace Transform Data Obtained by Dynamic Light Scattering. *Collect. Czech. Chem. Commun.* **1995**, 60, 1781–1797.
- (48) Stockmayer, W. H.; Schmidt, M. Effects of Polydispersity, Branching and Chain Stiffness on Quasielastic Light Scattering. *Pure Appl. Chem.* **1982**, 54 (2), 407–414.
- (49) Wu, C.; Zhou, S. Thermodynamically Stable Globule State of a Single Poly(N-Isopropylacrylamide) Chain in Water. *Macromolecules* **1995**, 28 (15), 5388–5390.
- (50) Johnson, L. M.; Li, Z.; LaBelle, A. J.; Bates, F. S.; Lodge, T. P.; Hillmyer, M. A. Impact of Polymer Excipient Molar Mass and End Groups on Hydrophobic Drug Solubility Enhancement. *Macromolecules* **2017**, *50*, 1102–1112.
- (51) Li, Z.; Johnson, L. M.; Ricarte, R. G.; Yao, L. J.; Hillmyer, M. A.; Bates, F. S.; Lodge, T. P. Enhanced Performance of Blended Polymer Excipients in Delivering a Hydrophobic Drug through the Synergistic Action of Micelles and HPMCAS. *Langmuir* **2017**, 33, 2837–2848.
- (52) Dalsin, M. C.; Tale, S.; Reineke, T. M. Solution-State Polymer Assemblies Influence BCS Class II Drug Dissolution and Supersaturation Maintenance. *Biomacromolecules* **2014**, *15*, 500–511.
- (53) World Health Organization. 21st WHO Model List of Essential Medicines; WHO, 2019.
- (54) Kasim, N. A.; Whitehouse, M.; Ramachandran, C.; Bermejo, M.; Lennernäs, H.; Hussain, A. S.; Junginger, H. E.; Stavchansky, S. A.; Midha, K. K.; Shah, V. P.; Amidon, G. L. Molecular Properties of

- WHO Essential Drugs and Provisional Biopharmaceutical Classification. *Mol. Pharmaceutics* **2004**, *1* (1), 85–96.
- (55) de Gennes, P. G. A Second Type of Phase Separation in Polymer Solutions. C. R. Adad. Sci., Ser. II Mec., Phys., Chim., Sci. Terre Univers 1991, 313 (10), 1117–1122.
- (56) Turner, K.; Zhu, P. W.; Napper, D. H. Coil-to-Globule Transitions of Interfacial Copolymers in Better than Theta-Solvents. *Colloid Polym. Sci.* **1996**, *274* (7), 622–627.